Journal of Theoretical and Applied Information Technology
15th October 2022. Vol.100. No 19

ISSN: 1992-8645 www.jatit.org E-ISSN: 1817-3195

DEEPREPOMEDUNM: A TRAIN DEEP LEARNING NETWORK AND EXTRACTION FEATURE FOR THE CLASSIFICATION OF PAP SMEAR IMAGES

DWIZA RIANA[1] , SRI HADIANTI[2], SRI RAHAYU[3], FARUQ AZIZ[4], FRIEYADIE[5], OEMIE KALSOEM[6]

[1,4]Computer Science, Universitas Nusa Mandiri, Faculty of Information technology, Indonesia

[2,3]Informatics, Universitas Nusa Mandiri, Faculty of Information technology, Indonesia

[5]Infromation System, Universitas Nusa Mandiri, Faculty of Information technology, Indonesia

[6]Laboratorium Medik Khusus Patologi Anatomik Veteran, Indonesia

E-mail: dwiza@nusamandiri.ac.id

ABSTRACT

The Pap smear test is still the best method for early detection of cervical cancer and preventing the fatal occurrence of cancer in women. Routine examinations can be carried out immediately to detect pre-cancerous lesions and take treatment measures. Although the Pap smear test is a superior test, it still has a weakness in the form of high false positive results due to human negligence. Advances in technology allow the use of deep learning and identification of cell features to classify Pap smear cells. Pap smear cells were acquired to produce Pap smear images. In the process, it generated multiple datasets like RepoMedUNM. The purpose of this study was to classify two classes and four classes of cells consisting of Normal class and three Abnormal classes, namely L-sil, H-sil, and Koilocyt. DeepRepoMedUNM is a classification process that uses VGG16, VGG19, Alexnet, ResNet50, and Euclidean distance methods on 60 Pap smear cell image features. The classification results obtained were compared and analyzed for two classes and four classes. For the RepoMedUNM dataset, we have obtained up-to-date classification accuracy of 96% for two-class and 91% four-class classification using VGG16 model.

Keywords: *Cervical Cancer, Classification, Ensemble Learning, Feature Fusion, Deep Learning, Pap Smear, Late Fusion Cervical Cell*

1. INTRODUCTION

WHO data in 2020 stated that around 342,000 women died from more than half a million who were affected by cervical cancer. Most of these incidents occur in poor countries. Death can be avoided and prevented by implementing a rapid and accurate screening program so that women with cervical disease get the care which they need in a timely and planned manner [1].

The Pap smear test needs to be done routinely by women over 30 years old to prevent cervical cancer effectively and to allow for early treatment and prevention [2]. Until now, the Pap smear test or liquid-based cytology is still the most popular screening technique to identify cervical cell abnormalities [3]. Cytologists perform a Pap smear test by taking a sample of cells from the cervical squamocolumnar and examining them through a light microscope to determine the level of malignancy of the cells [4],[5].

There are weaknesses in the manual cell examination system which is still difficult to carry out, takes a long time to observe, is tedious, and is prone to errors in identifying millions of cells in one slide with cell conditions that sometimes overlap. Therefore, it is necessary to develop an automatic computerized system that can effectively and efficiently analyze Pap smear cells. Computer-aided commercial products such as AutpPap300, PapNet, AutoCyte, Cytoanalyzer, CYBEST etc are technological advances in medical imaging that have better medical image quality and for early diagnosis of disease although they still have limitations because they still produce too many false positive rates, failure to detect low-grade abnormalities, and uncertainty over cost-effectiveness [6].

The use of classification techniques such as Deep Learning (DL) in the identification of abnormal Pap smear images is an attempt to overcome the limitations in early diagnosis of cervical cancer. Various kinds of DL have been used in Pap smear image classification studies, such as VGG16 [7],[8],[9],[10], VGG19 [11],[12], ResNet50 [8],[9],[13], ConvNet [8], and AlexNet [12],[14],[15] which have been used and resulted in a good classification of Pap smear images [11].

Our previous study [16] used the DL model in four classes, including normal, L-Sil, H-Sil, and Koilocyt in the RepoMedUNM dataset by segmenting K-means for texture feature cells. The Convolutional Neural Network (CNN) implements the pre-trained VGG16, VGG19, and ResNet50 models for the classification of three classes namely ThinPrep, non-ThinPrep and all data sets. In addition, the reuse pre-trained network method was used for the evaluation of the classification results.

This study is a continuation of [16] where there are quite significant differences in the dataset used, which consists of two classes and four classes of cells consisting of the Normal class and three Abnormal classes, namely L-sil, H-sil, and Koilocyt where the differences between each class has been recognized by a Pathologist. We will then refer to this dataset as the new RepoMedUNM dataset. There are differences in the number of cell images and the number of single cell Pap smears, namely 765 of 100 single cell images from Normal images, 1194 single cells from 100 L-Sil images, 547 single cells from 100 koilocyt images, and 750 single cells from 100 H-Sil images. In addition, we also added the AlexNet model and carried out extraction and classification for 30 features, with the aim of getting a comparison of the accuracy of each of the five model classifications and 30 feature classifications.

Pap smear image identification system with feature classification is carried out in various ways. One of them is a three-step method consisting of cell segmentation (cytoplasm, nucleus), feature extraction, and classification. In this system, pre-processing aims to improve image quality. Research with this method is still being carried out today where the cell nucleus is extracted using the super-pixel method [7], K-means [17], or clustering [18]. The next stage is segmented nuclear repair. After that, feature extraction is performed. Research on Pap smear images has extracted 20 features [19] and 26 features [11], namely intensity texture features and shape features extracted from segmented nuclei. Furthermore, the feature selection technique aims to get the most discriminant feature. At the last stage, a classifier is designed to classify cells [20]. In this study, we use additional 4 features as a continuation of the research [11] so that it can generate new information for the RepoMedUNM dataset.

The results obtained from the research phase on the new dataset RepoMedUNM achieved the highest classification accuracy respectively 96% and 91% for the classification problem of two classes and four classes using the VGG16 method while the feature classification obtained an accuracy of 71% for two classes and 56% for the four classes.

The main contributions of this paper are as follows: (1) classifying the new RepoMedUNM dataset. (2) Four types of CNN VGG16, VGG19, AlexNet, and ResNet50 were introduced to extract complementary features from various network depths. (3) As far as we observed, the feature extraction that we carried out was quite complete with 30 Pap smear cell image features consisting of intensity texture features and shape features for the nucleus and cytoplasm for a total of 60 features. (4) The comparison of the results of the DL model classification accuracy and the feature classification accuracy shows the highest accuracy value in model classification accuracy, which shows the potential for improvement of the cervical cancer diagnostic system.

The rest of the writing of this research is structured as follows: Sec. 2 discusses materials and methods. The materials section discusses the RepomedUNM dataset, the specific review literature of relevant DL, and the study of the features used in Pap smear image analysis, followed by an explanation of the stages of the research method. Sec 3 discusses the research results obtained from each stage of the research and its analysis. sec. 4 discusses all research results. The last part, Sec. 5 concludes this paper and opportunities for further research..

2. MATERIALS AND METHODS

2.1. Material

2.1.1. Dataset of RepomedUNM

Several collections of cervical cancer images and their retrieval techniques are discussed in this sub-chapter. The first collection in our previous research [16] was the RepoMedUNM database image from two types of Pap smear cells, namely ThinPrep and non-ThinPrep (conventional) as many as 6,168 Pap smear images with distribution as shown in table X. In the next collection, we collected cervical cancer images as many as 765 From 100 single cell images from Normal images, 1194 single cells from 100 L-Sil images, 547 single cells from 100 koilocyt images, and 750 single cells from 100 H-Sil images as shown in table Y. The dataset collection obtained is the result of digitizing images using an optical OLYMPUS microscope CX33RTFS2 and a microscope X52-107BN with a Logitech camera. Our goal is to provide a new dataset to expand the investigation of Pap smear images. A significant difference from the image display in the three classes of L-Sil, H-Sil, and Koylocy is that the new dataset already has very specific cells and the possibility of mixing with normal cells is very small.

In this study, classification was carried out on New RepoMedUNM with two scenarios. The first scenario is a classification for two classes, namely the Normal class consisting of 100 images with 765 cells and the Abnormal Class as many as 300 images with a total of 2491 cells. While the second scenario is a classification for four classes, namely Normal, L-Sil, Koilocyt, and H-Sil with a total each cell can be seen in Table 2.

Table 1. Distribution of RepomedUNM Dataset [16]

Category		Number of Images
Non Thinprep	Normal	3083
	L-Sil	818
Thinprep	Normal	1513
	Koilocyt	434
	H-Sil	410
Total		6168

Table 2. Distribution of New RepomedUNM Dataset

Category		Number of Images	Number of Cells
	Normal	100	765
	L-Sil	100	1194
Thinprep	Koilocyt	100	547
	H-Sil	100	750
Total		400	3256

2.1.1. DL Model and Pap Smear Image Features

The classification process of cervical cells can use the DL model design. DL model classification process was performed by extracting image features. Previous researchers used VGG16 to classify cervical cell images by including image features into machine learning classifications such as Support Vector Machine (SVM), Random Forest, and AdaBoost. They see that SVM performs better than other ML classifiers. An in-depth CNN-based (AlexNet base) feature extraction method with unattended feature selection was applied [21].

A CNN-based classification approach is to classify cervical cells, to apply the VGG16 and ResNet architectures, and to find that ResNet50 is more suitable than VGG16 based on its performance [9]. The pre-trained AlexNet architecture was used to extract cervical cell characteristics and to apply these features to classify them using SVM [22]. AlexNet, GoogleNet, ResNet, and DenseNet based on a pre-trained and fine-tuned CNN architecture were used to classify cervical cells [14] where cytoplasmic and nuclear segmentation is required for this method. Deep transfer learning-based classification approach to classify cervical cells into healthy and abnormal [8] with augmentation of previous data and patch extraction work [23]. The research applied deep transfer learning techniques based on AlexNet to detect, segment and classify cervical cells and demonstrated that segmentation was not required for classification.

In addition to the studies above, the VGG-like network consists of seven layers using pre-segmented cervical cells to perform the classification [22]. A comparative study was conducted based on five DL models, ResNet101, DenseNet161, AlexNet, VGG19, and SqueezeNet to examine their classification performance on cervical datasets where DenseNet161 provided maximum accuracy [12]. The features of the pre-trained Inception-V3, ResNet152, and InceptionResNetV2 were combined for analyzing biomedical images [24].

RepomedUNM image classification [16] has used the same 3 DL models as used in this study, namely VGG16, VGG19, and Resnet50. In this research, we added Alexnet DL model.

Table 3. Various Datasets and Feature Types

No	Dataset	Jumlah Fitur	Fitur
1	Herlev [19]	20	Nucleus area, Cytoplasm area, N/C ratio, Nucleus brightness, Cytoplasm brightness, Nucleus shortest diameter, Nucleus longest diameter, Nucleus elongation, Nucleus roundness, Cytoplasm shortest diameter, Cytoplasm longest diameter, Cytoplasm elongation, Cytoplasm roundness, Nucleus perimeter, Cytoplasm perimeter, Nucleus position, Maxima in nucleus, Minima in nucleus, Maxima in Cytoplasm, and Minima in cytoplasm.
2	SiPakMed [11]	26	Characterizing the intensity, the texture, and the shape of the cell and cytoplasm, total 54 features.
3	RepoMedUNM [16]	6	Metric features, Eccentricity, Contrast, Correlation, Energy, and Homogeneity.
4	New dataset RepoMEDUNM	30	Contras channel R, Contras channel G, Contras channel B, Intensity channel R, Intensity channel G, Intensity channel B, Area, Major axis length, Minor axis length, Eccentricity, Orientation, Equivalent Diameter, Solidity, extent, Smoothness, Entropy, Uniformly, Third moment channel R, Third moment channel G, Third moment channel B, Circularity, Euler number, Perimeter, and ConvexArea. Our features are available for cell and cytoplasm, total 60 features.

Cell features in Pap smear images play an important role in the process of identifying cell abnormalities. Observations of the features in the datasets of Herlev [19], Sipakmed [11], and RepomedUNM [16] indicated that it is possible to generate new features as an attempt to recognize the nucleus and cytoplasm of cells.

Table 3 shows that the research conducted [19] produced 20 features. These 20 features were used to test 7 classes of Pap smear images contained in the Herlev dataset using the linear least-squares classifier method and resulted in an average value of Oe% of 7,9%. Research [11] resulted in 26 features where these 26 features were used to test 5 classes of Pap smear images contained in the SiPakMed dataset using the Support Vector Machine (SVM), Multi-layer perceptron (MLP), and Convolutional Neural Network (CNN) methods with the highest accuracy values using the CNN method of 95.35%. Research [16] produced 6 features where these 6 features were used to test four classes of Pap smear images contained in the RepoMedUNM dataset using VGG16, VGG19, ResNet50 with the highest accuracy value using the ResNet50 method of 98.8%.

2.2. Method

Figure 1 is the flow of our DeepRepoMedUNM model. It can be seen that first, Pap smear images were taken from a dataset that can be accessed in the RepoMedUNM repository and used as training data where the details of the dataset can be explained in sec 4. Second, the pre-processing step is resizing and data augmentation for every 100 images contained in each class. Third, the dataset was processed using the DL model, which consists of VGG16, VGG19, AlexNet, and ResNet50 for the classification of two classes and four classes. Fourth, automatic cropping of single cells was carried out on the training data. Fifth, feature extraction was carried out on the cropped image, so it produced 30 features consisting of intensity texture features and shape features. Sixth, Euclidean Distance calculations were performed on 30 features to obtain accuracy values for two classes and four classes of Pap smear cell images. Seventh, evaluation of the matrix from the DL results and the results of the Euclidean distance was carried out so as to produce the values of accuracy, precision, recall, and F-score.

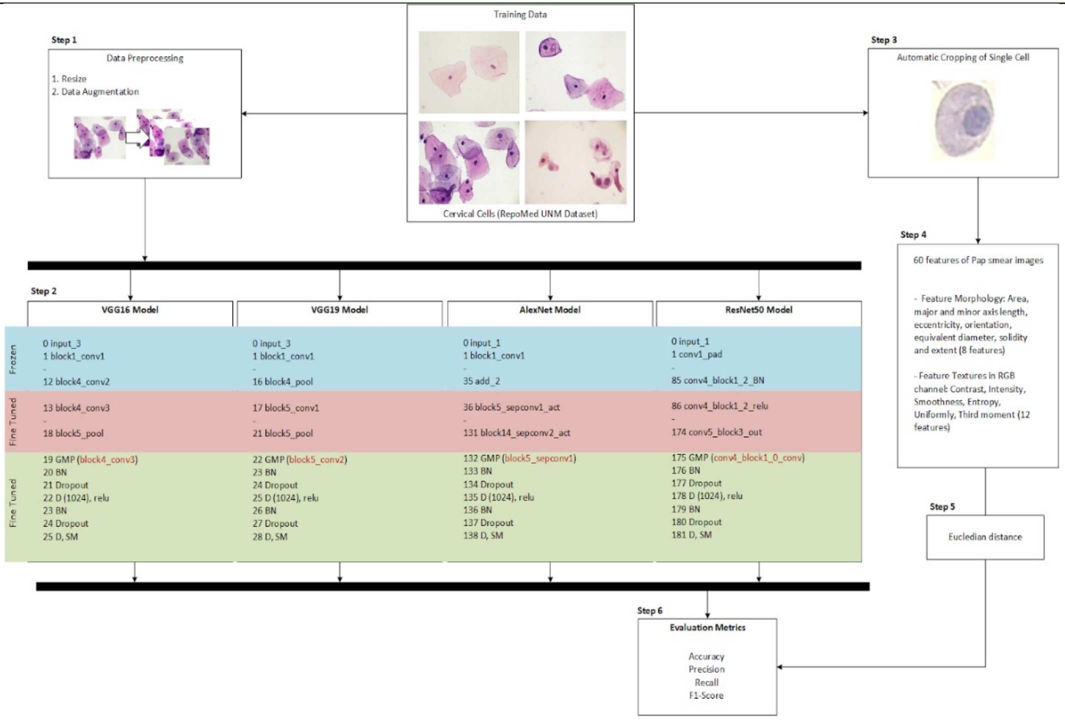

Fig 1. Research Flow Of The Train Deep Learning Network And Extraction Feature For The Classification Of Pap Smear Images

2.2.1. Data Pre-processing

1. Resize

The image from RepoMedUNM used in this study is in jpg format with a size (3264x2448). We resized the image scale to (227x227). The next step we did dynamic size detection according to cell size.

2. Augmentation Image

A total of 400 images with 100 images from the normal class, 100 images from the H-sil class, 100 images from the L-sil class, and 100 images from the Koilocyt class with 3267 cells were augmented to produce 1200 augmented images to be continued with the DL process. The augmentation process was carried out in three ways, namely reflection, translation, and scale which were carried out randomly. We believe that with the number of images and the number of cells increased by three times, the number of images is sufficient for the use of the VGG16, VGG19, ResNet50 and AlexNet DL models.

2.2.2. Classification with Four DL Models

The Pap smear image classification stage was carried out by processing the dataset using the DL model, which consists of VGG16, VGG19, AlexNet, and ResNet50 for the classification of two classes and four classes.

A large amount of data and high computations are usually required to train CNN. It also requires a longer training time. Many researchers use Transfer Learning (TL) as a solution. The concept of TL does not require learning from scratch, but it starts from learning patterns that have been learned and creates an accurate model [25],[26].

TL has a two-stage process. The first stage is to select a pre-training model. The model is trained on a large-scale benchmark dataset, according to the problem to be solved. The second stage is the refinement of the model with the size criteria and the similarity of the dataset with the previously trained model.

For the DL models of VGG series selected in the experiment are the AlexNet and ResNet50 networks in the TL process where the weights were pre-trained on the ImageNet dataset. There are 1.2 million training data called imageNet, 50,000 validation images, and a total of 100,000 test images which have 1000 classes [27].

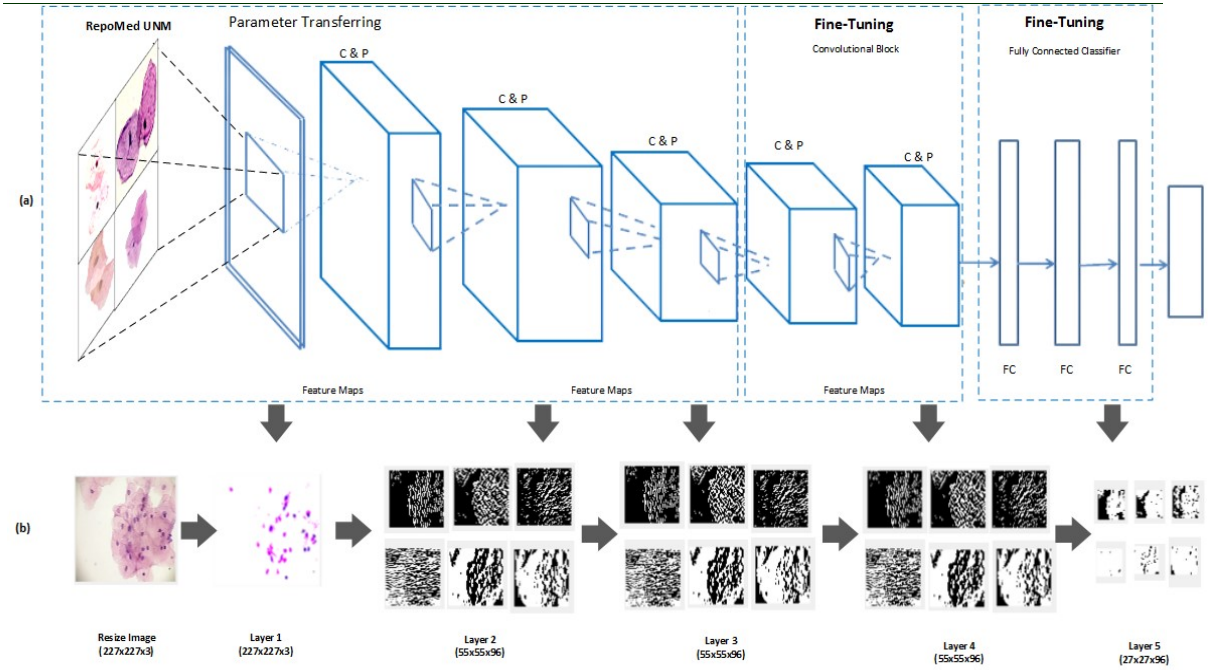

Fig 2. Visualization Of TL Process In Model DL VGG

For example, Figure 2 is a VGG16 model in which the first few convolution blocks use the transferred parameters (w1, w2, w3 …, wk) from another VGG16 network trained on the ImageNet dataset. For the four CNNs, the input size is (227 × 227 × 3), the learning speed for 6 epochs with a learning speed of 0.0003, the batch size in the test set uses a size of 10, and the optimager uses the Stochastic Gradient Descent with Momentum (SGDM).

Figure 2-(a) is the TL process on the VGG network. ImageNet data is used to train the first layer, and the last convolution block along with the FCL is fine-tuned. The bottom section shows the distribution of representative feature maps extracted from various convolution blocks of the VGG-16 network. This is an illustration that TL is able to extract information from the image. Figure 2 part a is where parameters are transferred from another CNN and fine-tuned on cervical cancer cell dataset (convolution (C), pooling (P), fully connected layer (FC)). Section b shows the Visualization of the feature maps of three different convolutional layers of VGG16.

2.2.3 Automated Cropping

The need for automated cropping in this study is mainly used to obtain 30 features of the nucleus and cytoplasm. The image has a collection of cells whose conditions sometimes overlap. We use automated cropping of about 30x30 of the input image size of 270x270. The results of the automated cropping image can be seen in Fig 3.

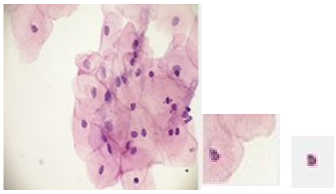

Fig 3. Visualization of Automated Cropping Results on Normal Class Images

2.2.4. Feature Extraction

At this stage, feature extraction was carried out on the cropped image so as to produce 30 features consisting of intensity texture features and shape features. In full, we counted for the cell nucleus and cytoplasm to obtain a total of 60 features. The calculated feature values are R channel contrast, G channel contrast, B channel contrast, R channel intensity, G channel intensity, B channel intensity, Area, Major axis length, Minor axis length, Eccentricity, Orientation, Equivalent Diameter, Solidity, extent, Smoothness, Entropy, Uniformly, Third moment R channel, Third moment G channel, Third moment B channel, Circularity, centroid, Perimeter, and Convex Area.

2.2.5 Feature Processing with Euclidean Distance

Processing and calculation of Euclidean Distance was carried out for 60 features to obtain accuracy values in the classification of two classes and four classes of Pap smear cell images. A simple calculation was performed to find the proximity of two vectors between features. Furthermore, this value is compared with the ground truth data that has been generated at the feature extraction stage.

2.2.6 Evaluation Metrics

In the final stage of the method, evaluation of the matrix from the results of the DL model classification and the results of feature classification were carried out. The evaluation was carried out so as to produce accuracy, precision, recall, and F1-score values from two classes and 4 classes. The calculations use the formula in Table 4.

3. RESULTS

The test results of 5 DL classification models were obtained in Table 5 where the classification results of the 5 applied models can be seen in Table 5. Of the four classification models applied to two classes and four classes from the dataset group, the results show that the VGG16 classification model has the highest accuracy value when compared to other models. VGG16 in data processing of two classes has an accuracy value of 96% and in four classes of 91% It can be concluded that the VGG16 model was successfully used on the New RepoMedUNM dataset. In Figure 4, we present a confusion matrix for all the classification models used. All the results shown can be seen that there are still difficulties in classifying all classes containing L-Sil cells. This creates new opportunities for researchers to evaluate with different classification models.

Table 4. Formula Of Evaluation Metrics

Assessments	Formula
Precision, P	$\frac{TP}{TP + FP}$
Recall, R	$\frac{TP}{TP + FN}$
F1- Score	$2x\frac{P\ x\ R}{P + R}$
Accuracy	$\frac{TP + TN}{TP + TN + FP + FN}$

Table 5. The Test Results Of 5 DL Classification Models

Type of Classification	CNN Model	Precision	Recall	F-1 Score	Accuracy
2- Class	VGG16	0.86	1	0.93	0.96
	VGG19	0.66	1	0.80	0.87
	AlexNet	0.64	1	0.78	0.86
	ResNet50	0.64	1	0.78	0.86
	60 Features	0.55	0.71	0.62	0.71
4-Class	VGG16	0.93	0.91	0.90	0.91
	VGG19	0.74	0.75	0.73	0.75
	AlexNet	0.85	0.85	0.84	0.85
	ResNet50	0.80	0.81	0.79	0.81
	60 Features	0.39	0.41	0.40	0.56

The classification model used produces a good classification and is neither overfitting nor underfitting. All can be seen because all the accuracy values are lower than the training accuracy values. This is also supported by a graphical display that shows the visualization of the classification results carried out in 2 classes. Figure 5 shows the classification accuracy generated from the CNN VGG16 model of 96%. Furthermore, the accuracy results generated from the CNN VGG19 model is 87% as shown in Figure 6. Meanwhile, the CNN AlexNet model produces a greater accuracy of 86% as shown in Figure 7, and the highest accuracy is generated by the CNN ResNet50 model of 86% as shown in Figure 8.

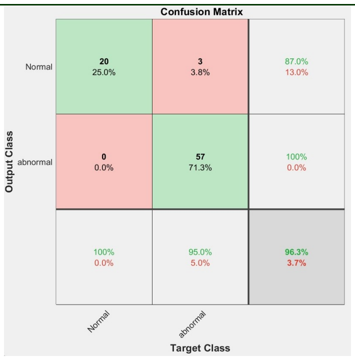

	Normal	abnormal	
Normal	20 25.0%	3 3.8%	87.0% 13.0%
abnormal	0 0.0%	57 71.3%	100% 0.0%
	100% 0.0%	95.0% 5.0%	96.3% 3.7%

a(1)

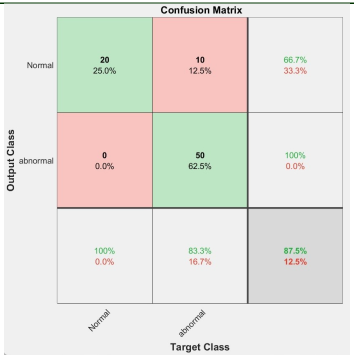

	Normal	abnormal	
Normal	20 25.0%	10 12.5%	66.7% 33.3%
abnormal	0 0.0%	50 62.5%	100% 0.0%
	100% 0.0%	83.3% 16.7%	87.5% 12.5%

a(2)

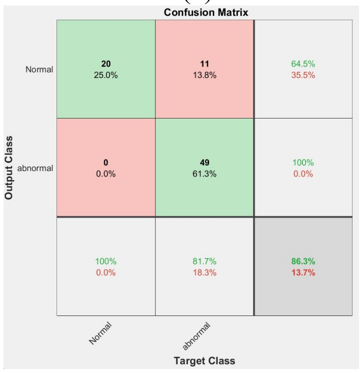

	Normal	abnormal	
Normal	20 25.0%	11 13.8%	64.5% 35.5%
abnormal	0 0.0%	49 61.3%	100% 0.0%
	100% 0.0%	81.7% 18.3%	86.3% 13.7%

a(3)

	Normal	abnormal	
Normal	20 25.0%	11 13.8%	64.5% 35.5%
abnormal	0 0.0%	49 61.3%	100% 0.0%
	100% 0.0%	81.7% 18.3%	86.3% 13.7%

a(4)

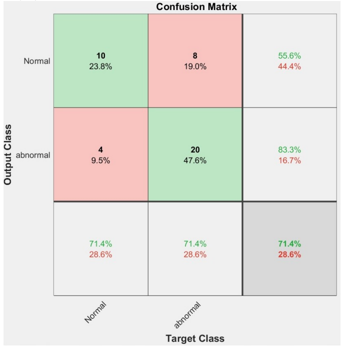

	Normal	abnormal	
Normal	10 23.8%	8 19.0%	55.6% 44.4%
abnormal	4 9.5%	20 47.6%	83.3% 16.7%
	71.4% 28.6%	71.4% 28.6%	71.4% 28.6%

a(5)

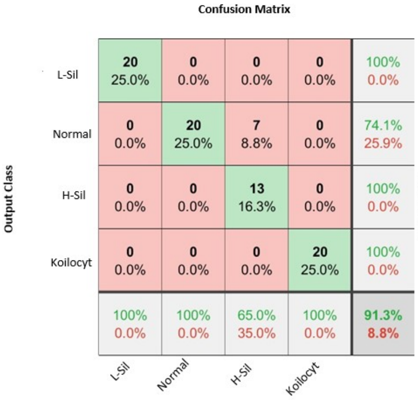

	L-Sil	Normal	H-Sil	Koilocyt	
L-Sil	20 25.0%	0 0.0%	0 0.0%	0 0.0%	100% 0.0%
Normal	0 0.0%	20 25.0%	7 8.8%	0 0.0%	74.1% 25.9%
H-Sil	0 0.0%	0 0.0%	13 16.3%	0 0.0%	100% 0.0%
Koilocyt	0 0.0%	0 0.0%	0 0.0%	20 25.0%	100% 0.0%
	100% 0.0%	100% 0.0%	65.0% 35.0%	100% 0.0%	91.3% 8.8%

b(1)

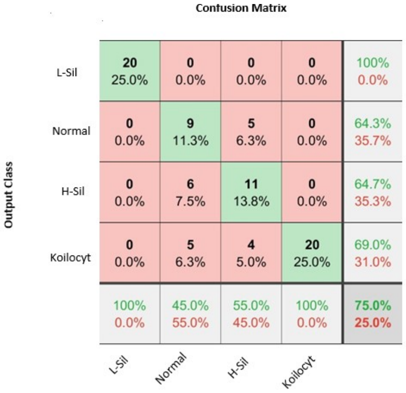

	L-Sil	Normal	H-Sil	Koilocyt	
L-Sil	20 25.0%	0 0.0%	0 0.0%	0 0.0%	100% 0.0%
Normal	0 0.0%	9 11.3%	5 6.3%	0 0.0%	64.3% 35.7%
H-Sil	0 0.0%	6 7.5%	11 13.8%	0 0.0%	64.7% 35.3%
Koilocyt	0 0.0%	5 6.3%	4 5.0%	20 25.0%	69.0% 31.0%
	100% 0.0%	45.0% 55.0%	55.0% 45.0%	100% 0.0%	75.0% 25.0%

b(2)

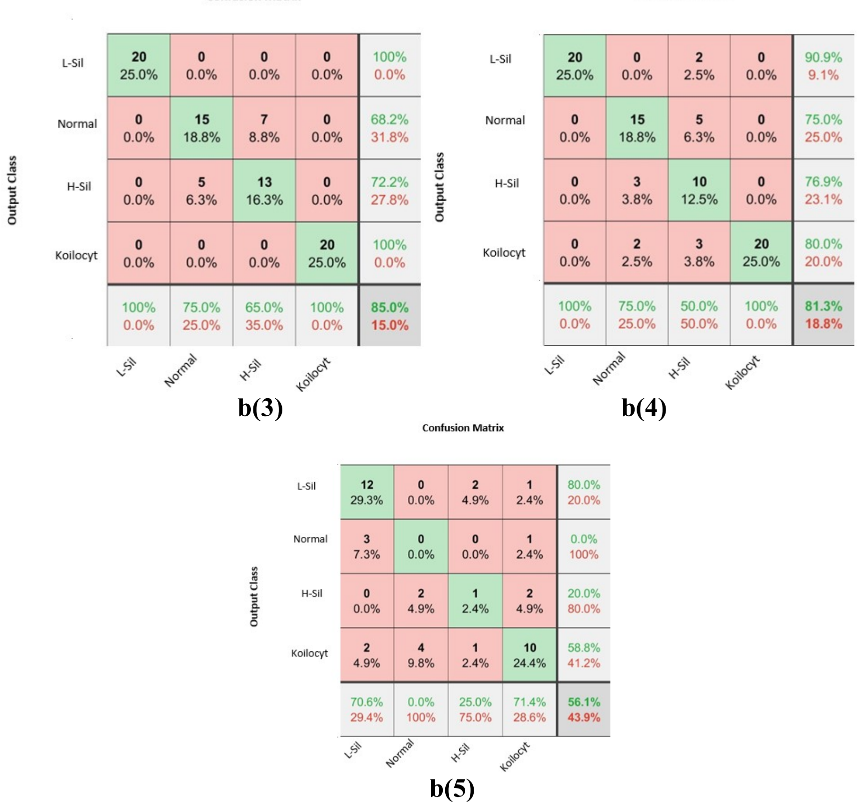

Confusion Matrix

Output Class	L-Sil	Normal	H-Sil	Koilocyt	
L-Sil	20 25.0%	0 0.0%	0 0.0%	0 0.0%	100% 0.0%
Normal	0 0.0%	15 18.8%	7 8.8%	0 0.0%	68.2% 31.8%
H-Sil	0 0.0%	5 6.3%	13 16.3%	0 0.0%	72.2% 27.8%
Koilocyt	0 0.0%	0 0.0%	0 0.0%	20 25.0%	100% 0.0%
	100% 0.0%	75.0% 25.0%	65.0% 35.0%	100% 0.0%	85.0% 15.0%

b(3)

Confusion Matrix

Output Class	L-Sil	Normal	H-Sil	Koilocyt	
L-Sil	20 25.0%	0 0.0%	2 2.5%	0 0.0%	90.9% 9.1%
Normal	0 0.0%	15 18.8%	5 6.3%	0 0.0%	75.0% 25.0%
H-Sil	0 0.0%	3 3.8%	10 12.5%	0 0.0%	76.9% 23.1%
Koilocyt	0 0.0%	2 2.5%	3 3.8%	20 25.0%	80.0% 20.0%
	100% 0.0%	75.0% 25.0%	50.0% 50.0%	100% 0.0%	81.3% 18.8%

b(4)

Confusion Matrix

Output Class	L-Sil	Normal	H-Sil	Koilocyt	
L-Sil	12 29.3%	0 0.0%	2 4.9%	1 2.4%	80.0% 20.0%
Normal	3 7.3%	0 0.0%	0 0.0%	1 2.4%	0.0% 100%
H-Sil	0 0.0%	2 4.9%	1 2.4%	2 4.9%	20.0% 80.0%
Koilocyt	2 4.9%	4 9.8%	1 2.4%	10 24.4%	58.8% 41.2%
	70.6% 29.4%	0.0% 100%	25.0% 75.0%	71.4% 28.6%	56.1% 43.9%

b(5)

Fig 4. A. (1) Confusion Matrix For 2 Class With VGG16 (2) VGG19, (3) Alexnet, (4) Resnet50, (5) 60 Features. B. (1) Confusion Matrix For 4 Class With VGG16 (2) VGG19, (3) Alexnet, (4) Resnet50, (5) 60Features

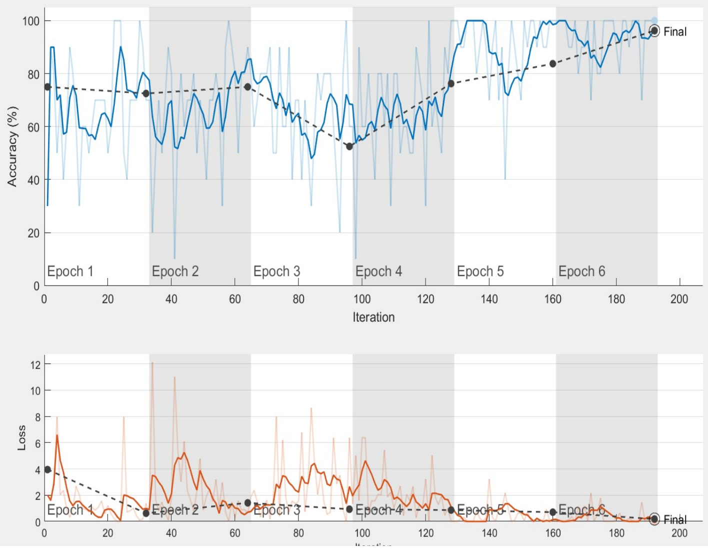

Fig 5. Graph Of Accuracy And Loss Curve VGG16

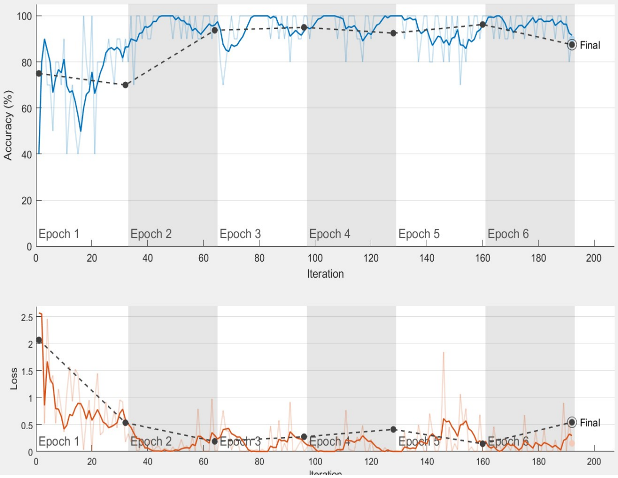

Fig 6. Graph Of Accuracy And Loss Curve VGG19

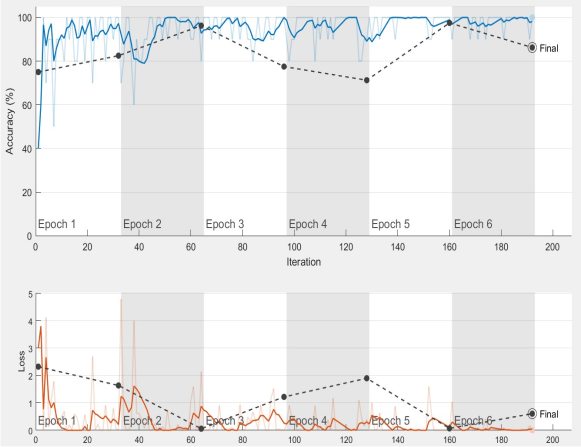

Fig 7. Graph Of Accuracy And Loss Curve Alexnet

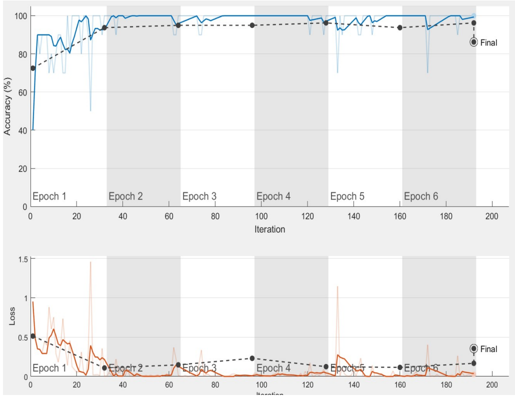

Fig 8. Graph Of Accuracy And Loss Curve Resnet50

The texture feature extraction presented in our dataset which can be seen in Fig 9 is a graph of the 60 feature values. The features in our dataset can then be used as data to do a number of things, including those related to image analysis. The features can also be an alternative in doing learning in differentiating between classes for early detection of cervical cancer.

In order to find out the distribution of the mean values for the 60 generated features, we present them in a graph representing the 54 mean values of the nuclear and cytoplasmic features. You can see the difference in the average value and the feature pattern on the two lines. In Figure 10, 6 features are not shown because of the large difference in the average values, namely Uniform red nucleus (15101.46), Uniform green nucleus (12490.88), Uniform blue nucleus (14664.88), Circularity nucleus (12788.71), ConvexArea cytoplasm (2046.88), and, Area cytoplasm (1946.05).

The graph of the average feature values shows that the highest average value lies in the red intensity feature of the nucleus, while the low average value is found in the cytoplasmic EulerNumber feature, the cytoplasm red third moment, and the cytoplasm blue third moment. These results can be useful for analysis and identification of Pap smear cell images and can be studied further.

Figure 11 is an example of 4 cell images derived from the prediction results of the classification with the DL model where the cell image has a value of 100%, meaning it has been successfully recognized. The value of 72.9% and 59.7%, even though it is not 100%, it turns out that the class prediction results are still correct.

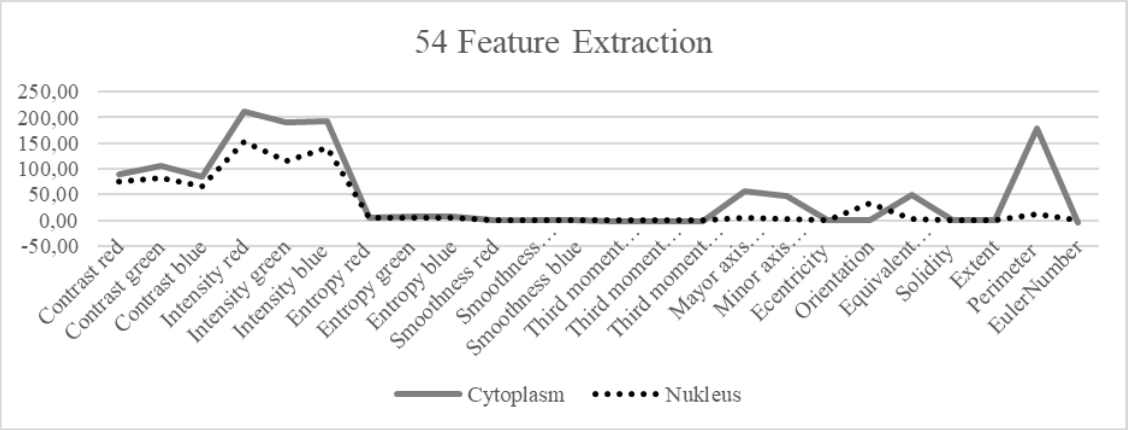

Fig 10. Feature Graphics Of All Cells

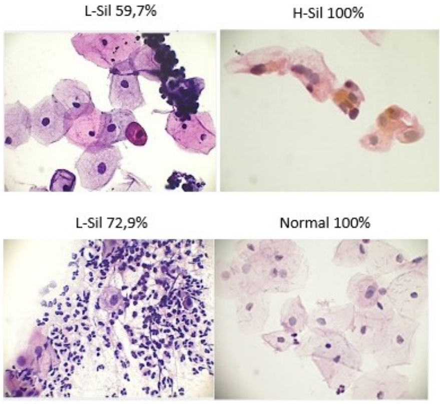
L-Sil 59,7%
H-Sil 100%
L-Sil 72,9%
Normal 100%

Fig 11. L-Sil Image Detected L-Sil Of 59.7%, L-Sil Image Detected L-Sil Of 72.9%, H-Sil Image Detected H-Sil Of 100%, Normal Image Detected Normal Of 100%

4. DISCUSSION

The use of classification techniques such as DL in the identification of abnormal Pap smear images is an effort to overcome the limitations in early diagnosis of cervical cancer. This research is called DeepRepoMedUNM in cervical cell classification from the New RepoMedUNM dataset, and from this research, complete results were obtained regarding the train deep learning network and extraction feature for the classification of Pap smear images.

Model structure, number of epochs, dataset distribution, loss function, image quality, complexity, and optimization function are important factors and can affect the performance of a model [27]. We observe the confusion matrix for the New RepoMedUNM dataset in Table 5. For the scenario of the classification of two classes, namely normal and abnormal classes and the classification of four classes, namely Normal, H-sil, Koilocyt, and L-sil classes using the ResNet50 model, the performance is relatively good compared to VGG16, VGG19, and AlexNet. Thus it can be concluded that the shallow network performs better than the deep network in the RepoMedUNM dataset.

Figure 10 is an example of 4 cell images derived from the prediction results of the classification with the DL model where the cell image has a value of 100%, meaning it has been successfully recognized. The value of 72.9% and 59.7%, even though it is not 100%, it turns out that the class prediction results are still correct.

Another work carried out in this study, we extracted features on 5 classes of cervical cancer images and generated 60 features from the nucleus and cytoplasm. From the feature accuracy results, we divided the existing data into training data to produce features that will be stored in the database as benchmark features whose class is already known, and test data that will compare its features later with the training data features which already exist in the database. In the future, further research needs to be done to obtain the features of the nucleus and cytoplasmic cells from Pap smear images.

5. CONCLUSIONS

The RepoMedUNM database provides data for the cell image analysis community to research not only for the classification process but also for the evaluation of image segmentation techniques for single cells, group cells, or overlapping cells. There are four categories of these cells, namely normal cells, L-Sil, Koilocyt, and H-Sil which were identified by pathologists. A total of 60 features of the nucleus and cytoplasm of the five classes are provided. As a continuous reference from the initial evaluation of 6 features and for the evaluation of various techniques in the future for image classification of cervical cancer cells, CNN classification is applied. Furthermore, DeepRepoMedUNM is a classification process using the VGG16, VGG19, Alexnet, ResNet50, and Euclidean distance methods on 60 Pap smear cell image features, intensity texture, and shape features for the nucleus and cytoplasm respectively. The comparison on the results of the DL model classification accuracy and the feature classification accuracy shows the highest accuracy value at 96% for 2 classes, namely normal and abnormal using the DL VGG16 model, and the highest accuracy for the four classes, which is 91% using VGG16, which indicates the potential for improvement of the diagnostic system of cervical cancer. The RepomedUNM database will continue to grow. The image acquisition process is carried out continuously. On the other hand, data analysis is becoming more widely open and poses a challenge for researchers who are interested in this field of medical imagery.

Funding: This research received no external funding.

Data Availability Statement: Not applicable.

Acknowledgments: The authors would like to thank the national competitive applied research grant of the Directorate General of Higher Education, Ministry of Education, Culture, Research, and Technology for supporting this research through “Repository Medical Imaging Pap Smear Images For Cervical Cancer Research In Indonesia Early Detection Of Cervical Cancer”, 2022. The authors would like to thank the Lab Medik Khusus Patologi Anatomik Veteran Indonesia for the resource of RepoMedUNM database

Conflicts of Interest: The authors declare no conflict of interest

REFERENCES

[1] WHO, “New recommendations for screening and treatment to prevent cervical cancer,” 2021. https://www.who.int/news/item/06-07-2021-new-recommendations-for-screening-and-treatment-to-prevent-cervical-cancer

(accessed Jun. 27, 2022).

[2] S. A. Francis *et al.*, "A qualitative analysis of South African women's knowledge, attitudes, and beliefs about HPV and cervical cancer prevention, vaccine awareness and acceptance, and maternal-child communication about sexual health," *Vaccine*, vol. 29, no. 47, pp. 8760–8765, 2011, doi: 10.1016/j.vaccine.2011.07.116.

[3] L. A. Liang, T. Einzmann, A. Franzen, K. Schwarzer, and G. Schauberger, "Cervical Cancer Screening : Comparison of Conventional Pap Smear Test , Liquid-Based Cytology , and Human Papillomavirus Testing as Stand-alone or Cotesting Strategies Cervical Cancer Screening : Comparison of Conventional Pap Smear Test , Liquid-Based Cy," no. November 2020, 2022, doi: 10.1158/1055-9965.EPI-20-1003.

[4] G. N. Papanicolaou, "New Cancer Diagnosis," *Third Race Betterment Conf.*, 1928.

[5] N. Papanicolaou, G and H. Traut, F, "The Diagnostic Value of Vaginal Smears in Carcinoma of the Uterus." Archives of pathology & laboratory medicine, 1997.

[6] P. B. Shanthi, K. S. Hareesha, and R. Kudva, "Automated Detection and Classification of Cervical Cancer Using Pap Smear Microscopic Images : A Comprehensive Review and Future Perspectives," pp. 20–41, 2022.

[7] R. R. P. A. C. Kavida, "Extracting the cervical cancer cell region through super pixel segmentation," *J. Ambient Intell. Humaniz. Comput.*, 2021, doi: 10.1007/s12652-021-03259-w.

[8] L. Zhang, L. Lu, I. Nogues, R. M. Summers, S. Liu, and J. Yao, "DeepPap: Deep convolutional networks for cervical cell classification," *IEEE J. Biomed. Heal. Informatics*, vol. 21, no. 6, pp. 1633–1643, 2017, doi: 10.1109/JBHI.2017.2705583.

[9] H. Wieslander *et al.*, "Deep Convolutional Neural Networks for Detecting Cellular Changes Due to Malignancy," *Proc. - 2017 IEEE Int. Conf. Comput. Vis. Work. ICCVW 2017*, vol. 2018-Janua, pp. 82–89, 2017, doi: 10.1109/ICCVW.2017.18.

[10] P. Hridayami, I. K. Gede, D. Putra, and K. S. Wibawa, "Fish Species Recognition Using VGG16 Deep Convolutional," vol. 13, no. 3, pp. 124–130, 2019.

[11] M. E. Plissiti *et al.*, "Sipakmed : A New Dataset For Feature And Image Based Classification Of Normal And Pathological Cervical Cells In Pap Smear Images," *2018 25th IEEE Int. Conf. Image Process.*, pp. 3144–3148, 2018.

[12] Y. Promwors, S. Pattanasak, C. Pintavirooj, and W. Piyawattanametha, "Comparisons of Pap smear Classification with Deep Learning Models," in *Proceedings of the 14th Annual IEEE International Conference on Nano/Micro Engineered and Molecular Systems*, 2019, pp. 282–285.

[13] D. Riana, D. H. Widyantoro, and T. L. Mengko, "Extraction and classification texture of inflammatory cells and nuclei in normal pap smear images," *Proc. - 2015 4th Int. Conf. Instrumentation, Commun. Inf. Technol. Biomed. Eng. ICICI-BME 2015*, pp. 65–69, 2016, doi: 10.1109/ICICI-BME.2015.7401336.

[14] H. Lin, "Fine-Grained Classification of Cervical Cells Using Morphological and Appearance Based Convolutional Neural Networks," *IEEE Access*, vol. 7, pp. 71541–71549, 2019, doi: 10.1109/ACCESS.2019.2919390.

[15] J. Amin *et al.*, "Integrated Design of Deep Features Fusion for Localization and Classification of Skin Cancer," *Pattern Recognit. Lett.*, 2019, doi: 10.1016/j.patrec.2019.11.042.

[16] D. Riana, "RepoMedUNM : A New Dataset for Extraction Feature and Train Deep Learning Network to Classify of Pap Smear Images."

[17] H. Hafeez and L. Guoliang, "Image Processing Approach for Segmentation of WBC Nuclei based on K-Means Clustering," pp. 175–181.

[18] P. Chen *et al.*, "Chronic Lymphocytic Leukemia Progression Diagnosis with Intrinsic Cellular Patterns via Unsupervised Clustering," 2022.

[19] J. Jantzen, J. Norup, G. Dounias, and B. Bjerregaard, "Pap-smear Benchmark Data For Pattern Classification," *Proc. NiSIS 2005, Albufeira, Port.*, no. November, pp. 1–9, 2005.

[20] K. Y. Win, S. Choomchuay, K. Hamamoto, M. Raveesunthornkiat, L. Rangsirattanakul, and S. Pongsawat, "Computer aided diagnosis system for detection of cancer cells on cytological pleural effusion images," *Biomed Res. Int.*, vol. 2018, 2018, doi: 10.1155/2018/6456724.

[21] K. Bora, M. Chowdhury, L. B. Mahanta, M. K. Kundu, and A. K. Das, "Pap smear image classification using convolutional neural network," *ACM Int. Conf. Proceeding Ser.*, 2016, doi: 10.1145/3009977.3010068.

[22] Kurnianingsih *et al.*, "Segmentation and classification of cervical cells using deep learning," *IEEE Access*, vol. 7, pp. 116925–

116941, 2019, doi: 10.1109/ACCESS.2019.2936017.

[23] S. Gautam, K. K. Harinarayan, N. Jith, A. K. Sao, A. Bhavsar, and A. Natarajan, “Considerations for a PAP Smear Image Analysis System with CNN Features,” pp. 1–8.

[24] L. D. Nguyen, R. Gao, D. Lin, and Z. Lin, “Biomedical image classification based on a feature concatenation and ensemble of deep CNNs,” *J. Ambient Intell. Humaniz. Comput.*, vol. 0, no. 0, p. 0, 2019, doi: 10.1007/s12652-019-01276-4.

[25] M. Raghu, “Transfusion : Understanding Transfer Learning for Medical Imaging,” no. NeurIPS, 2019.

[26] S. J. Pan and Q. Yang, “A Survey on Transfer Learning,” vol. 22, no. 10, 2010.

[27] M. M. Rahaman *et al.*, “DeepCervix: A deep learning-based framework for the classification of cervical cells using hybrid deep feature fusion techniques,” *Comput. Biol. Med.*, vol. 136, no. July, p. 104649, 2021, doi: 10.1016/j.compbiomed.2021.104649.